# Energy Harvesting and Wireless Data Transmission System for Rotor Instrumentation in Electrical Machines

Danilo X Llano*[1], Salman Abdi[2], Mark Tatlow[3], Ehsan Abdi[4], Richard A McMahon[5]

[1]Danilo X Llano was with the Electrical Engineering Division, University of Cambridge, 9 JJ Thomson Avenue, Cambridge CB3 0FA, UK. He is currently with WMG, University of Warwick, Coventry CV4 7AL, Coventry, UK
[2]Salman Abdi was with the Electrical Engineering Division, University of Cambridge, 9 JJ Thomson Avenue, Cambridge CB3 0FA, UK. He is currently with WMG, University of Warwick, Coventry CV4 7AL, Coventry, UK
[3]Mark Tatlow was with the Electrical Engineering Division, University of Cambridge, 9 JJ Thomson Avenue, Cambridge CB3 0FA, UK. He is currently with McLaren Automotive Ltd.
[4]Wind Technologies Limited, St Johns Innovation Park, Cambridge CB4 0WS, UK
[5]WMG, University of Warwick, Coventry CV4 7AL, Coventry, UK

*danilo.llano@gmail.com / dxl20@cantab.net

## Abstract

It is desirable to measure rotor quantities such as currents and temperatures in an electrical machine for design verification and condition monitoring purposes. A Bluetooth module which sends data from the rotor was previously reported in literature, but this module was battery powered, and therefore the duration of the tests was limited. This paper presents a solution to this problem by developing a rotor-mounted power supply system which can harvest energy from the magnetic field inside the machine, by fixing an external loop to the rotor and making use of the induced voltage in the loop. A full-bridge rectifier, boost converter and battery charging module was developed to supply sufficient power to a bespoke Bluetooth transmission system and associated sensor circuitry.

## 1. Introduction

The ever increasing use of variable speed drives (VSD) in both traditional industries and in new areas such as the automotive sector, robotics and more electric ships and aircraft has led to a need for electrical machines with high performance, reliability, robustness, efficiency and power density. Achieving successful machine designs requires a good knowledge of machine parameters, especially thermal parameters, for the prediction of performance but their determination and verification are difficult, especially for rotor-related quantities.

Unfortunately, rotor measurements cannot be wired out to a data acquisition system without great difficulty, thus any signal must be transmitted wirelessly. A battery powered system to measure rotor currents and transmit the data using Bluetooth has been reported [1, 2]. In that approach

the batteries required regular recharging and the system had to be partially dismounted from the rotor to be charged, which limits the practicality of the instrumentation system and the tests than can be carried out. On the other hand, when the drive is in operation, there is a potential source of energy in the magnetic field of the machine that could be used to feed low power instrumentation, but achieving stable DC power from this field is challenging due to its variable frequency and amplitude.

This present paper describes an energy harvesting module which draws power from the magnetic field in an electrical machine and transmits rotor data wirelessly via Bluetooth to a data acquisition tool based on LabVIEW. The system has been implemented in a brushless doubly fed machine (BDFM), where the presence of two separate stator windings with different pole numbers and supply frequencies, and a special rotor winding design, creates an advantageous magnetic field distribution for energy harvesting [3]. Also, the BDFM used in this work has been extensively studied in [4] so the data acquired with the rotor instrumentation system can be confirmed against previous simulation and experimental results. Although the system has been demonstrated in a BDFM, most of the electronic designs and control algorithms are applicable or easily extendable to other machines. The approach also opens possibilities for the long term condition monitoring of machines.

The current prototype has been designed to be as small as possible but its physical size is still rather big for small machines or machinery with high power density. Bearing this in mind, there are two main target applications: using this instrumentation in large size machines with enough room to accommodate the system or looking at design verification of prototypes where it is practical to extend the shaft to accommodate the module, noting that this may alter the thermal behaviour of the machine.

Instrumentation to measure rotor temperatures in electrical machines has been reported in the literature as part of thermal modelling studies or the verification of sensorless temperature estimators and observers [5, 6, 7, 8]. In all cases, those systems were battery powered and transmitted data wirelessly using infrared (IR) communication [5, 6]. The authors in [9] used an isolated DC/DC converter IC connected to the synchronous machine excitation to feed temperature sensors and a Bluetooth data transmission system. Another energy harvesting technique using a small DC generator and an attached eccentric mass was proposed in [10, 11]. The armature of the DC generator is attached to the prime mover rotor and field magnets are held in a frame free to rotate relative to the rotor. A small mass is also attached to the frame so that it remains stationary as the rotor/armature spins but the mass will be displaced so that a gravitational torque equal to the DC generator torque (in steady state conditions) is established. The reported arrangement uses a maximum power point tracking algorithm (MPPT) to maximise the power extracted from the DC generator i.e. when the load and armature resistances are equal. The system has an energy conversion stage composed of a boost converter to perform the MPPT algorithm and a buck converter to regulate the DC link at 3.3 V. The system was characterised on a test bench and generated about 60 mW at 2000 rpm [10]. This solution has limited power and requires a DC generator, energy conversion and energy storage circuitry leading to a complex system with large volume.

Battery powered solutions are relatively attractive if only temperature measurements are required since low sampling rates are acceptable and the Bluetooth and analogue circuitry can operate in energy saving mode. On the other hand, batteries are not particularly suitable if rotor currents are also measured because higher sampling and data transmission rates are required to record waveforms (0-200 Hz) with a reasonable resolution and the circuitry will be operating in an active mode most of the time, demanding more power. The energy harvesting and rotor instru-

mentation reported in this paper are in the form of modules that can be easily adapted to a final user's instrumentation requirements. For instance, the size of the energy harvesting module could be reduced if only temperature sensors are used since low power and hence less energy storage are demanded.

This paper is organised as follows: first at all, a suitable method for extracting energy from the BDFM rotor is investigated and calculations are carried out to determine the expected range of voltages and frequencies that this would yield. Other practical issues such as construction, ease of retro-fitting to the rotor, and mechanical reliability are also considered. Then, an energy conversion system which converts low AC input voltages from the machine rotor into a stable DC power supply suitable for feeding electronic systems is presented. A MOSFET based active rectifier is proposed for AC/DC conversion and voltage boosting. Later on, a current and temperature sensing, signal conditioning, Bluetooth data transmission system and its associated software are described. The system includes Rogowski coils for current measurements, PT100 probes for temperature sensing, amplifiers and analogue filters for signal conditioning, and a Bluetooth module and microcontroller for wireless communication. Finally, a data logger based on LabVIEW is presented for data management.

## 2. Overview of the BDFM and the machine measuring system

### *2.1. BDFM machine*

The brushless doubly-fed machine is a variable speed electrical machine which shows particular promise in applications such as wind energy generation or as a VSD, but still needs design and thermal modelling verification [12]. The BDFM has two separate stator windings, which must be of different pole numbers to avoid direct coupling between them. The machine of interest in this paper has a 4-pole winding connected directly to the 50 Hz 3-phase grid, and an 8-pole winding supplied via a power converter. The basic outline of the BDFM system is shown in Fig. 1 (left). The rotor, however, must couple to the two air gap fields associated with the two stator windings. The machine used in this paper has a nested-loop rotor; this is formed from sets of concentric copper bars. Fig. 1 (right) shows a view of the nested-loop rotor with six 'nests', and three loops per nest.

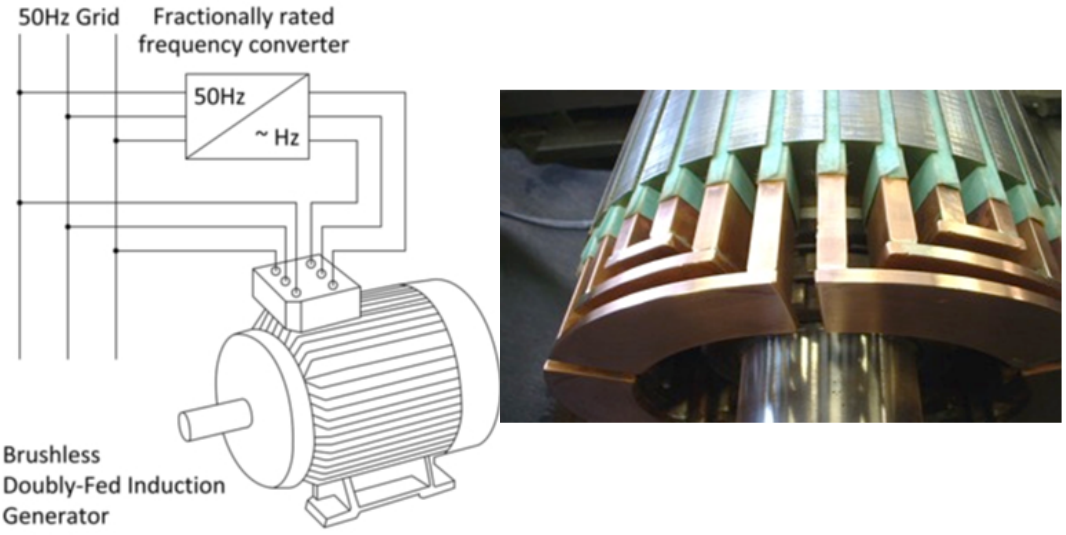


***Fig. 1.*** *Block diagram of the BDFM (left), End view of D180 nested-loop BDFM rotor (right)*

An experimental BDFM has been constructed in a frame size 180; its key specifications are given in Table 1. A rotor-mounted wireless system for measurement of the rotor bar currents and temperatures was initially designed by Abdi et al. in [13]. It used Rogowski coils [14] to measure the currents, and incorporated signal conditioning, analogue to digital conversion, and a Bluetooth module to transmit the measured data to a computer. The system was battery powered, but the life of the batteries was insufficient to perform tests of extended duration.

**Table 1** Specification of the 7.8 kW D180 BDFM

| Characteristic | General | Grid tied winding | Converter fed winding |
|---|---|---|---|
| Frame size | 180 | | |
| Poles | | 4 | 8 |
| Voltage rating | | 240 V at 50 Hz (delta) | 172 V at 25 Hz (delta) |
| Current rating | | 9.5 A (line) | 6.8 A (line) |
| Speed range | 750 rpm $\pm$ 33% | | |
| Rated torque | 100 Nm | | |
| Rated power | 7.8 kW at 750 rpm | | |
| Stack length | 0.19 m | | |
| Efficiency (at full load) | ˜92 % | | |

### *2.2. Rotor measuring system*

This electronic system requires a stable 6 V DC link to match the minimum input voltage necessary for a 5 V linear regulator. The later is used to achieve a good quality DC link for the electronic components. Subsequently, two different voltage levels are derived, 5 V for the energy harvesting module and gate drivers and 3.3 V for the Bluetooth module and analogue signal conditioning board. The current requirement was conservatively estimated based on analysis of the system. Table 2 lists the main elements of the system and their predicted contributions to the current draw, based on the maximum power consumption figures in the manufacturers' datasheets. Overall the energy harvesting system must be able to supply at least 200 mA at 6 V to power the measuring

system and electronics in the energy module itself. The 6 V DC link was selected based on the fact that the MOSFETs used in the active rectifier are optimized for 5 V applications and the system was developed in modules so that the power supply and the instrumentation/Bluetooth boards can be used independently if necessary. The later requires having a voltage regulator on each board. However, this design can be optimized according to the user specifications, for example, if only temperature measurements are required, the size, number of components and power consumption will be reduced significantly.

**Table 2** Power specification for the energy harvesting system

| Circuit element | Current (mA) |
|---|---|
| Bluetooth Module | 38 |
| Microcontroller | 20 |
| Rogowski Coil circuitry | 24 |
| Temperature sensor circuitry | 25 |
| Energy harvesting microcontroller | 24 |
| Power distribution system | 19 |
| **Total (including 33% margin)** | **200** |

## 3. Energy harvesting techniques

The energy harvesting system was designed to meet the specifications outlined in Table 3. The output current of 200 mA is the estimated maximum current consumption of the rotor instrumentation operating at 6 V (later reduced to 5 V or 3.3 V with a linear regulator).

Different methods of energy harvesting from rotor magnetic fields has been assessed based on analytical calculations to determine the expected voltages and frequencies that each option would yield. Other practical issues such as construction, ease of retro-fitting to an existing rotor and mechanical robustness were also considered. This analysis has been reported in [15] and it was concluded that a dedicated rotor loop, as described below, is the best option.

**Table 3** Specification for the rotor energy harvesting power supply

| Characteristic | Value |
|---|---|
| Input voltage range | 0.75-1.5 Vrms |
| Input frequency range | 20 - 50 Hz |
| Output voltage | 6 Vdc |
| Output current | 200 mA |
| Run time with no input power | 10 minutes |
| Temperature rating | 85 °C |

### *3.1. Energy harvesting rotor loop*

The energy harvesting loop is realised by making connections to two rotor bars which are pitched at the desired angle and shorted at one end through the end ring. The pitch angle can be chosen so that the energy harvesting loop couples with the magnetic field of either or both stator windings. A pitch angle of 90° is attractive because this will couple fully to the grid tied winding, see Fig. 2.

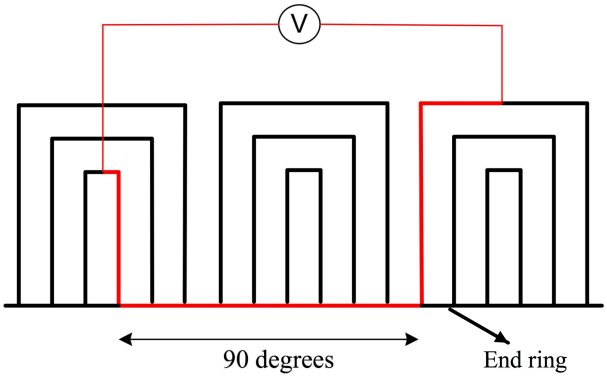


***Fig. 2.*** *Energy harvesting loop comprising two rotor bars pitched 90$^o$ apart and shorted at one end through an end ring. The rotor has 36 slots.*

Applying Faraday's law to the machine, the voltage $E_{rms}$ induced in a single loop that fully couples to the air-gap field $B_{rms}$ is given by:

$$E_{rms} = \frac{l\omega d}{p} B_{rms} \tag{1}$$

where $l$ is the stack length of the machine, $d$ is the air-gap diameter, $p$ is the number of pole-pairs for the relevant winding, and $\omega$ is the frequency in the rotor reference frame. In [16] the measured air-gap field of the 4-pole winding (grid tied with rated supply) was $0.30$ T$_{rms}$ at 230 V. The frequency $f$ in the rotor reference frame is given by

$$f = f_s - p\frac{2\pi N}{60} \tag{2}$$

where $f_s$ is the electrical frequency applied to the relevant stator windings, $p$ is the number of pole pairs for the relevant winding and $N$ is the mechanical speed of the rotor. Using (1), the voltage and frequencies expected in the external rotor loop are given in Table 4. This method has the advantage of being physically robust, in contrast to the end winding transformer, provided the wire taps are securely fastened to the rotor bars. However, the induced voltage is low and there is no possibility of using additional turns to increase this voltage, though a step up converter can be used to raise the voltage to a more useful level. Ultimately, this method was chosen due to its mechanical simplicity, despite its low output voltage levels.

### *3.2. Finite element analysis*

The induced voltage in a rotor loop can be also determined by Finite Element (FE) analysis. The D180 BDFM machine is modelled in synchronous mode at the full load specification listed in Table 1. Full load conditions were chosen for the FE analysis because they can be compared with the analytical calculations to validate the estimations done for sizing the energy harvesting module. Fig. 3 (left) shows the magnetic flux in the iron circuit with 4/8-pole stator winding configuration. A single-turn coil with a pitch angle of 90° is wound around the rotor slots through the machine stack length in the FE mesh to simulate the external loop formed from taps to the rotor bars, so

that coupling with the 8-pole air gap field is mainly eliminated. Fig. 3 (right) shows the induced voltage in the external rotor coil at different mechanical speeds. The rms value of the induced voltages obtained by FE are shown in Table 4. The voltages estimated analytically by Faraday's law and FE analysis are similar.

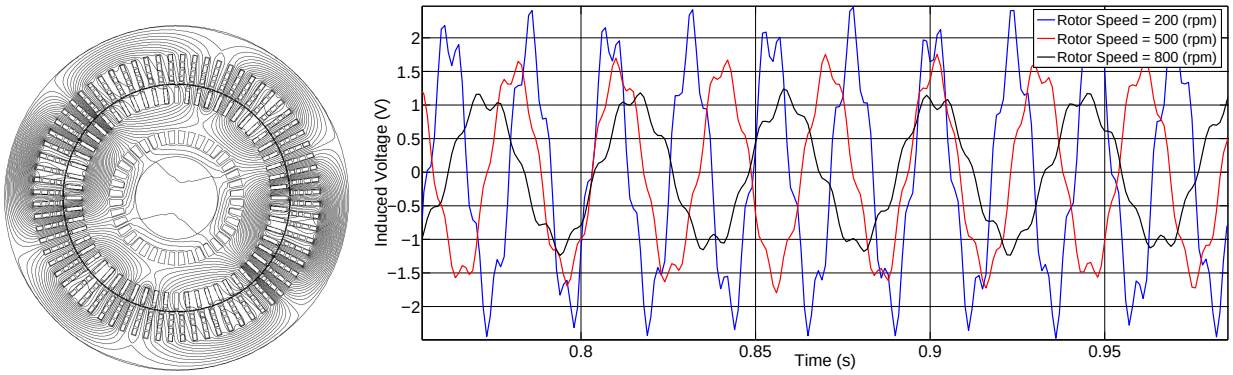


***Fig. 3.*** *Finite element analysis - Distribution of flux density in the D180 BDFM iron circuit in synchronous mode of operation (left), , Induced voltages in the additional loop mounted in rotor slots with a pitch angle of 90$^o$ (right)*

**Table 4** Voltage and frequencies induced in a single rotor loop of 90$^o$ pitch

| Rotor speed (rpm) | Electrical frequency (Hz) | Voltage (Vrms) - calculation | Voltage (Vrms) - FE |
|---|---|---|---|
| 200 | 43.3 | 1.39 | 1.49 |
| 500 | 33.3 | 1.07 | 1.12 |
| 800 | 23.3 | 0.75 | 0.79 |

## 4. Design of the energy conversion module

The system is designed to meet a list of specifications set out in Table 3. The energy harvesting module must operate in the challenging environment inside an electrical machine, where it will be subjected to high temperatures, strong magnetic fields, vibration and centripetal acceleration. These specifications include a moderate margin to allow for uncertainty over the precise characteristics of the machine.The energy conversion system must be designed to:

- Rectify and step-up the low AC input voltage from the rotor bars.
- Provide a small amount of energy storage to keep the system operating for short periods when the machine is idle.

Fig. 4 (top) shows the block diagram of the proposed solution.

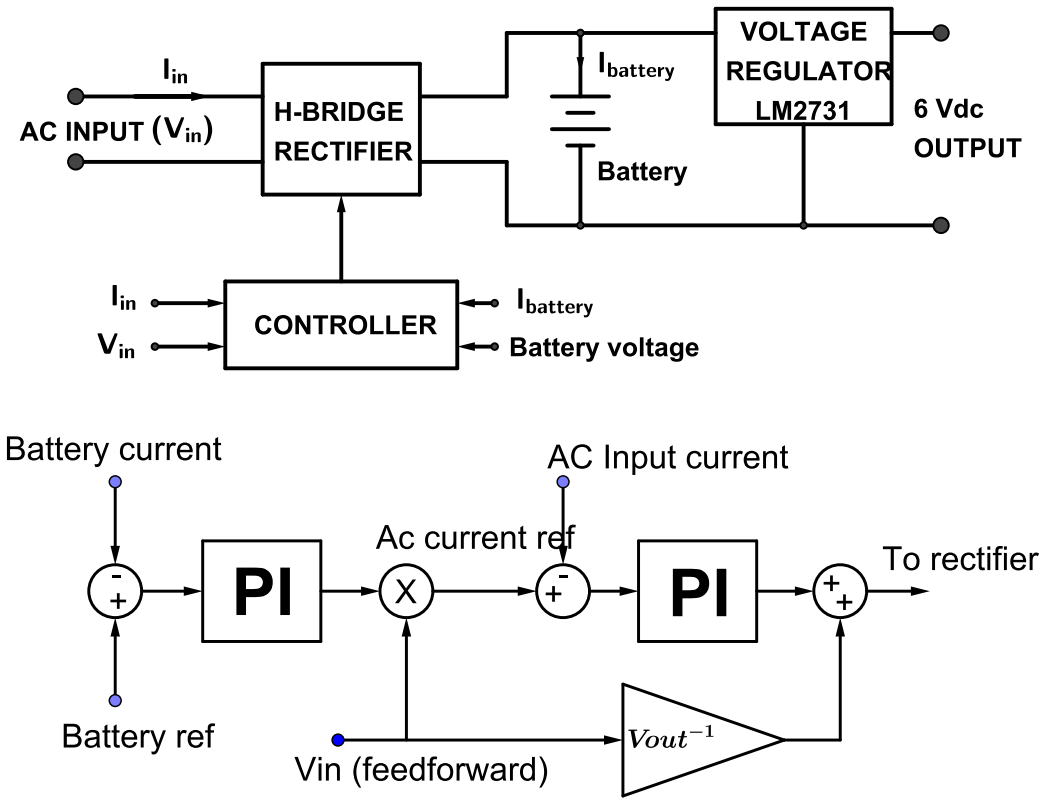


***Fig. 4.*** *Energy harvesting scheme (top), Control scheme (bottom)*

### *4.1. Rectifier*

A passive diode rectifier is not suitable due to the low input voltage as the voltage drop across the diodes would use up almost all of the available voltage, even if Schottky barrier diodes with low forward voltage were used. Therefore, a MOSFET based active rectifier (H Bridge) with additional line inductance was chosen for rectification and stepping up the DC voltage at the same time. The continuous output power requirement was conservatively estimated up to 1.5 W. It can be shown that if the effects of dead-time, MOSFET $R_{on}$ resistance, and other parasitic effects associated with PWM switching are neglected, the magnitudes of the rectifier input voltage and the DC link voltage are related as:

$$\alpha = \frac{V_{in}}{V_{DC}} \tag{3}$$

where $\alpha$ is a single parameter such that $|\alpha| < 1$. A closed-loop controller is necessary to deal with the variable input voltage and compensate for the elements that were neglected in (3).

A detailed circuit diagram of the proposed solution is shown in Fig. 5.

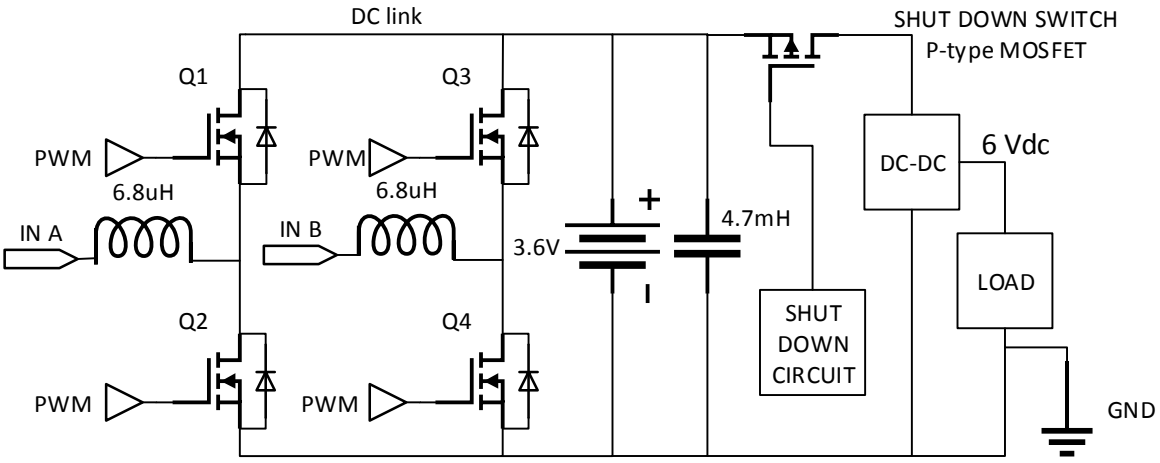


***Fig. 5.*** *Circuit diagram*

### *4.2. Energy storage*

Supplying 200 mA at 6 V for 10 minutes would require a total energy storage capacity of 720 J. However, it would be desirable to allow some additional margin in the design subject to space and weight constraints. This energy storage could be implemented either with a small rechargeable battery or using double-layer electrolytic capacitors. However, both of these technologies rely on chemical processes and are therefore temperature sensitive. Different battery options were considered and among them a Nickel-Metal Hydride rechargeable battery rated at 510 mAh and 3.6 V, about 1100 J in 10 minutes, was chosen to power the system when the rotor is idle. The battery can withstand a continuous trickle charge, so accurate charge management is not required. The battery is rated at 85°C, which is the maximum operating temperature recommended by the manufacturer. Unfortunately, batteries with a higher temperature rating were not available from manufacturers in a small quantity.

### *4.3. Output stage*

A DC/DC converter (LM2731) was selected to regulate the DC link at 6 V. This IC has embedded the main active elements for a standard boost converter (power MOSFET, gate driver, PWM controller, feedback amplifier and protection circuits) and is used with an external inductor, diode, capacitors and resistors, the latter for setting the output voltage. The switching frequency is 600kHz.

### *4.4. Shut down circuitry*

For practical use inside the machine it was required that the power supply could be shut down wirelessly, to switch off the measuring circuit and avoid draining the battery when the machine was not running. This was especially important since charge in the battery is needed in order for the power supply to start up. This cannot be done via the wireless system since the radio is powered down in the off state. A centripetal switch was considered, but the acceleration at minimum speed (200 rpm) was only about 2 g, making it difficult to distinguish from gravity depending on the

orientation of the switch. It was therefore decided to detect the presence of voltage at the input terminals and use this to trigger the power supply to start. The circuit in Fig. 6 was devised to sense this voltage and switch on the power supply. When $V_{AB} \geq 0.6$ V, the transistor $Q1$ turns on, pulling the gate of the P-MOSFET towards ground and allowing it to connect the battery to the output stage. The 10 k$\Omega$ resistor and 22 $\mu$F capacitor allow the gate voltage to remain low even during negative half-cycles of the input voltage, when the transistor is off. Furthermore, to allow operation to continue for periods while the machine is idle, a second transistor $Q2$ was added, with its base current controlled by the microcontroller. During normal operation, the microcontroller keeps this transistor turned on so the circuit will remain active. However, the microcontroller can be instructed to pull this pin low, turning off the transistor. If this occurs while the machine is inactive, both transistors will then be off, and the PMOS's gate voltage will rise due to the 10 k$\Omega$ resistor. This will turn off the power to the output stage, shutting down the system.

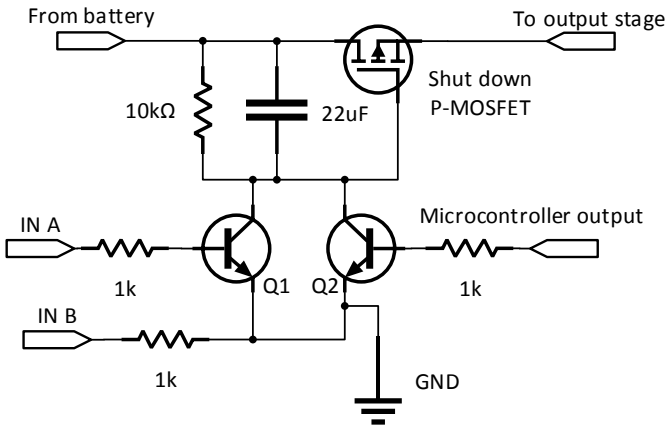


***Fig. 6.*** *Shut down circuitry*

### *4.5. Control system*

*4.5.1. Control structure:* A closed-loop controller is needed to regulate the power flow through the rectifier as the relationship between $\alpha$ in (3) and the output current is not straightforward. A control scheme with two nested PI controllers, an inner loop to regulate the input current within limits, and an outer loop to regulate the battery current is used. The block diagram of the proposed controller is given in Fig. 4 (bottom). RC low-pass filters were added to the sensor circuits to remove switching-frequency noise.

This strategy is similar to the control structure used for single phase active rectifiers with regulated DC link voltage [17, 18]. However, the presence of the battery introduces the need for using its charging current in the outer control loop. First at all, charging currents, rather than voltage figures, are commonly given in battery specifications. Second, it is highly desirable to control the charging current of the battery since this is the only way of ensuring that the battery will be sufficiently charged to power the system when the machine is not rotating. The system also measures the battery voltage, which in turn is used to identify any overcharging condition. The charging current would be set to zero in this later case.

The power balance equation is written as follows:

$$P_{AC} = P_{DC} \Longrightarrow V_{in} I_{in} = V_{DC} \left( I_{BAT} + I_{CAP} + I_{LOAD} \right) \tag{4}$$

Considering $I_{CAP} = C \frac{dV_{DC}}{dt}$, and $V_{DC} = V_{BAT} = I_{BAT} Z_{BAT}$, where $Z_{BAT}$ is the battery impedance, and (3) it is possible to write:

$$\alpha I_{in} = I_{BAT} + C \frac{d}{dt} \left( I_{BAT} Z_{BAT} \right) - I_{LOAD} \tag{5}$$

Eq. (5) shows that the battery current can be regulated by controlling the AC input current and $I_{LOAD}$ can be treat as a disturbance. $I_{LOAD}$ was varied for characterising of the module (efficiency measurements in section 5), but it was fairly constant during actual operation. Also, when the machine is running the load and any circuitry will be powered by the AC side and the current to the battery will be specifically used to charge the battery so that its stored energy can be used when the machine is idle, but the instrumentation is still operating, or to wake up the system. The DC/DC converter is represented by the $I_{LOAD}$ term in this analysis. Unfortunately, the manufacturer does not provide enough details to model this component. However, no stability issues were identified during characterization with loads that varied significantly more than the values expected for normal operation. In addition, the specifications for the DC/DC converter are given for an input of 2.7 V - 14 V and maximum load current of 1.8 A, which are within the operation range of the module.

*4.5.2. AC control (feed-forward loop):* It is well known that PI controllers cannot track sinusoidal references (as the input current) without a steady state error [19], but this limitation can be overcome by adding a feed-forward loop using the measured input voltage. In addition, to prevent instability when the peak of the output current is reached, a limit was placed on the maximum input current that could be requested by the outer loop. By applying this limit to the output of the outer PI controller, operation in the unstable regime beyond the point of maximum power transfer is avoided.

**Dynamic response:** Finally, some consideration must be given to the transient response of the control system. A formal mathematical analysis could be conducted, using techniques such as state space averaging to determine the transfer functions of the rectifier [20], but this is beyond the scope of this paper. Instead, the following general points were used to estimate appropriate values for the filter cut-offs and integrator time constants.

- The inner loop should have a phase lag as close as possible to zero over the whole AC input frequency range. This was necessary to maintain the power factor near unity.
- The outer loop should have low bandwidth to strongly attenuate the ripple in the battery current at twice the fundamental input frequency.
- The low-pass filter on the input current reading must pass the full range of input frequencies, but should strongly attenuate the switching frequency and its harmonics. The cut-off point must not be set too low to avoid limiting the response rate of the inner loop. The gains of the loops were adjusted by trial and error to obtain the desired response.

## 5. Construction and testing of the energy harvesting system

### 5.1. Construction

Results for the first energy harvesting prototype were reported in [15]. A second version of the system has been built and tested. The original prototype was built using three single PCBs (80 mm x 49 mm each one), while the new design has only two boards of the same size. This was achieved by using components with the smallest package, suitable for hand assembly, available in the market. Additionally, nexFET MOSFETs (CSD16321Q5) from Texas Instruments were used in an effort to minimise $R_{on}$ resistance (2.1 m$\Omega$ at $V_{GS}$=4.5 V from datasheet specifications), track resistance and parasitic inductances as the devices are packaged in SON (small-outline no leads) 5 mm x 6 mm packages. Having fewer boards also reduces losses due to connectors and wires between PCBs. The components are rated up to 125 $^{o}$C and automotive qualified if available. As already stated the limiting component is the battery. Heavier components such as inductors and the battery can be mechanically secured to the mounting bracket, but this was not done in the current prototype. The hexagonal bracket shown in Fig. 7 (left) has been designed to allow the energy harvesting boards, Bluetooth module and three other circuit boards (if required) to be secured to the rotor shaft. The two halves separate to allow fitting the whole unit onto the rotor shaft.

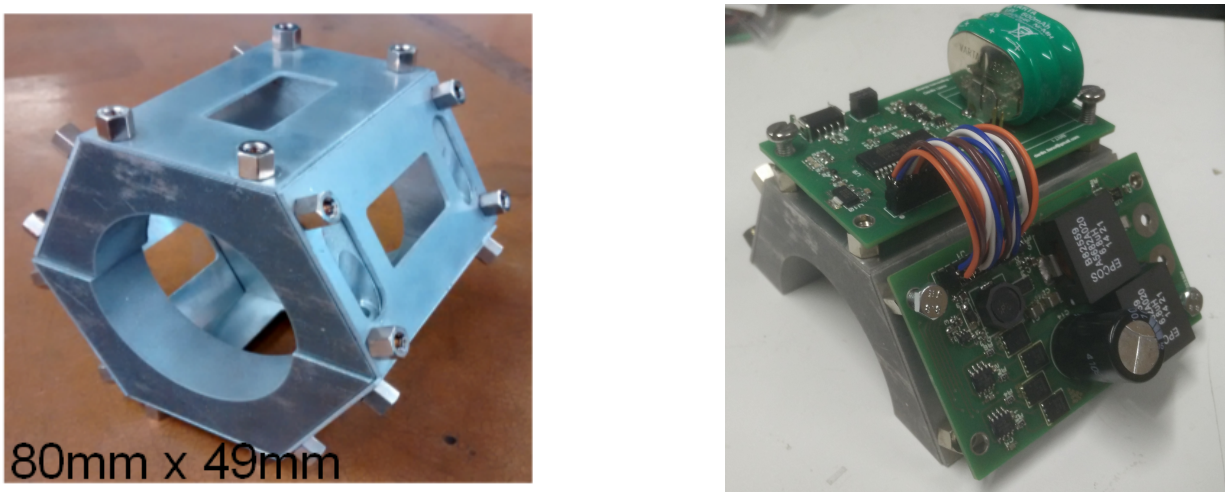


***Fig. 7.*** *Hexagonal bracket for mounting the circuit boards to the rotor shaft (left), Power electronics, energy storage and control PCB (right)*

### 5.2. General characteristics

A low cost AVR 8 bit microcontroller from Atmel was used to run the control algorithms detailed in subsection 4.5. Unipolar PWM at 25 kHz and 125 ns dead-time was used to drive the active rectifier. The MOSFETs and gate drivers were selected to operate at $V_{GS}$=5 V. The current consumption of the microcontroller was 39 mA, while the gate drivers, sensing amplifiers and voltage reference ICs require about 32 mA. These values are comparable with the estimates listed in Table 2. The charging current reference can be wirelessly set from the graphical interface described in section 6.3. The battery manufacturer recommends a trickle current between 5-15 mA for long term operation. A 25 mA reference value was used during characterization as this is the minimum current recommended for normal charging.

### 5.3. Maximum load current and efficiency tests

The second prototype of the energy harvesting module was characterised on the laboratory bench with a low voltage, variable frequency AC power supply as was done for the first system reported in [15]. The power source was composed of a signal generator and amplifier to achieve the power level required by the circuit. Later, in order to match the real rotor as closely as possible, it was necessary that the power source should have as low output impedance as possible. For this, a commercially available toroidal transformer with a third winding wound by hand through the toroid using thick wire is used. The measured output impedance of the circuit in this configuration is 83 m$\Omega$ over the full range of frequencies.

The battery current was set to 25 mA and the load was a variable resistor. The results presented here correspond to the first (in blue) and second prototype (in red) to show the improvement not only in size but also in performance. The maximum available load current is plotted in Fig. 8 (left). The 200 mA target was achieved at an input voltage of 0.74 V and 0.67 V for the first and second prototype respectively, which meets the specifications outlined in Table 3. Varying the input frequency from 20 to 50 Hz was found to have no measurable effect on performance. The efficiency of the modules is shown in Fig. 8 (right). The efficiency is calculated as:

$$\eta = \frac{P_{load} + P_{AR} + P_{bat}}{P_{AC}} \tag{6}$$

where $P_{AR}$ is the power required to feed the active rectifier circuitry (gate drivers, voltage references, etc), $P_{load}$ is the power consumed by the load (variable resistor in these tests, but the instrumentation and Bluetooth boards in the final implementation), $P_{bat}$ is the power required to charge the battery at 25 mA and $P_{AC}$ is the input power.

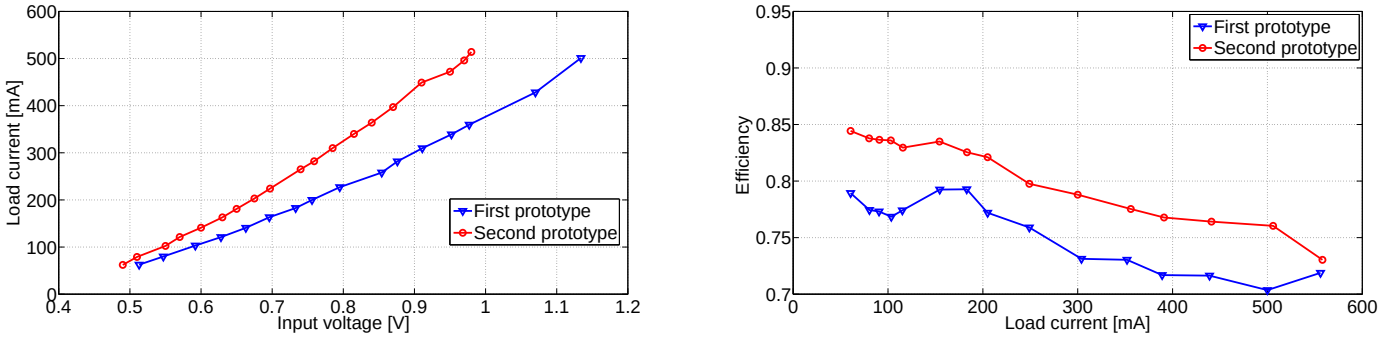


***Fig. 8.*** *Maximum load current delivered from the converter module over an input voltage range with a battery trickle charge of 25 mA (left). Efficiency of the converter module with a battery trickle charge of 25 mA (right)*

## 6. Bluetooth data transmission system for rotor instrumentation

Fig. 9 shows the block diagram of the rotor instrumentation and Bluetooth data transmission system.

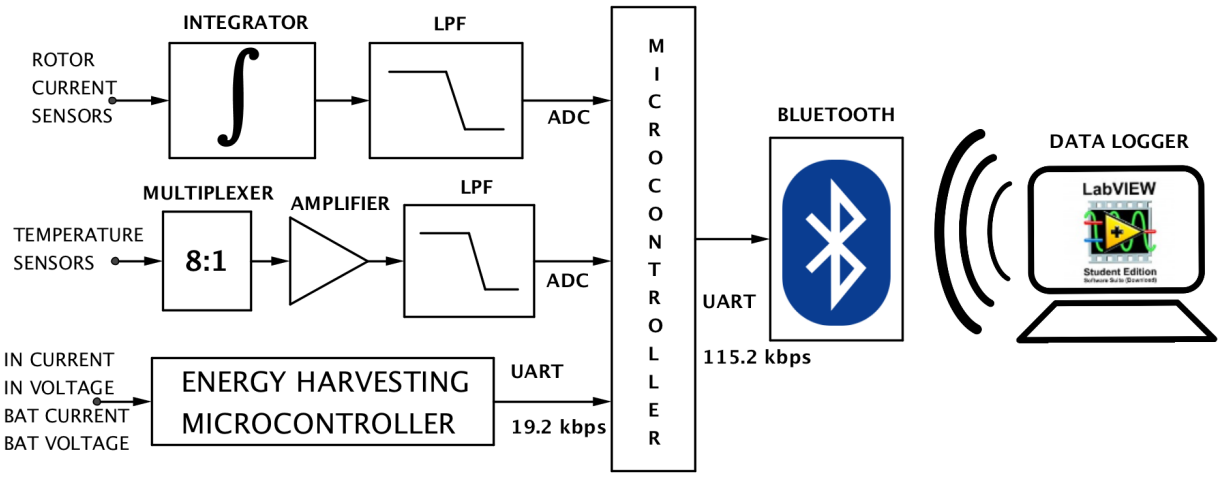


***Fig. 9.*** *Bluetooth system scheme*

### *6.1. Bluetooth module*

A WT12 Bluetooth 2.1 chip from Bluegiga Technologies is used for wireless data transmission. It has an integrated chip antenna, UART communication, 30 m range in line-of-sight and can be easily integrated with a microcontroller for a fully functional control and data transmission system. The microcontroller used for this task was a SAM4S from Atmel. This microcontroller manages the communication with the Bluetooth module, ADC sampling, temperature multiplexing, serial communication with the energy harvesting module to get data about the state of the battery (voltage and current), input voltage and input current. This system is built independently from the energy harvesting module to have modularity so that different transmission systems (with different sensors for example) can be integrated to the same power source.

### *6.2. Temperature, current sensors and signal conditioning*

*6.2.1. Temperature sensors :* PT100 temperature sensors rated at -50°C to 500°C were selected. The system has 8 temperature channels multiplexed with an 8:1 digitally controlled analogue switch CD74HC4051M96 from Texas Instruments. The sampling process is done as follows: the microcontroller selects the temperature channel to be connected to the output of the multiplexer and allows 250 ms to let the signal to settle. The resistance of the selected PT100 probe is sensed using a Wheatstone bridge configuration. Afterwards, this measurement is amplified ($gain = 100$) with an instrumentation amplifier (AD627BRZ from Analog Devices) and low pass filtered with a second order Sallen-Key filter with unity gain, $Q = 0.5$ and cut-off frequency 3.5 Hz. The same temperature channel is then sampled 50 times at 2 kHz and finally the average value is transmitted to the Bluetooth module. This process is repeated for all the channels under controlled by the LabVIEW user interface.

*6.2.2. Current sensors:* The Rogowski coils were manufactured as described in [13, 1] to measure the rotor currents. The voltage induced at the coil terminals is proportional to $di/dt$ rather than $i\,(t)$, therefore an integrator and low pass-filter are required for signal conditioning, in this case an analogue implementation. The rotor currents are expected to be within 20-1000 Arms and

0-200 Hz. Assuming a sinusoidal current $i = I \sin \omega t$, then the output voltage at the coil terminals will be

$$V_{coil} \quad = \gamma \frac{di}{dt} = \quad \gamma \omega I \cos \omega t \tag{7}$$

where $\gamma$ is the Rogowski coil constant and depends on its physical construction [13, 1].

A practical integrator circuit has a transfer function given by

$$\frac{V_{out}}{V_{in}} = -\frac{k_G}{j\frac{\omega}{\omega_n} + 1} \tag{8}$$

where $k_G$ is the integrator gain and $\omega_n$ is its natural frequency. Assuming $\omega \gg \omega_n$, then the magnitude of (8) can be approximated as

$$\left| \frac{V_{out}}{V_{in}} \right| \quad = \quad k_G \frac{\omega_n}{\omega} \tag{9}$$

If (7) is applied to (9), then the frequency term $\omega$ is effectively cancelled out, leading to a constant gain $k_G \omega_n$ regardless of the frequency. The integrator was designed with $\omega_n = 0.378$ rad/s (0.06 Hz) and $k_G = 1833$. The gain and natural frequency could be modified independently if required. The low pass filter is a Sallen-Key filter with gain $G = 1.6$, $Q = 0.707$ and cut-off frequency 5.3 kHz to maintain constant gain and almost zero phase shift in the frequency range 5 Hz -1 kHz as there is an interest in measuring the third and fifth harmonic components in the current waveform.

The system has four current channels. The microcontroller samples and stores 100 points for each channel. The sampling frequency is adapted in each data acquisition run to maintain good resolution and 400 data points are transmitted via Bluetooth. The LabVIEW interface calculates the frequency of the measured waveforms and sets the sampling frequency accordingly for the next iteration (at least 20 points per cycle).

### *6.3. LabVIEW data acquisition system*

A data logger based on LabVIEW was developed for data acquisition, processing and recording. This interface communicates wirelessly with the Bluetooth module using a serial protocol at 115.2 kbps. The program acquires temperature, rotor current and data from the energy harvesting module at different rates. The program also manages the communication, does all the numerical transformations (sampled signals from the ADCs at 12 bits to values with a physical meaning), displays the measurements in real time, calculates characteristics such as the DC offset (for self-calibration), the RMS value and frequency of the rotor current and records data for further analysis if required. The user interface is shown in Fig. 10 (top). It has all the communication settings on the left , information about the energy harvesting module in the centre, and rotor current and temperature measurements on the right. A second tab displays time trends for temperature and energy harvesting values.

### *6.4. Bench calibration*

Fig. 10 (bottom) shows the sensor and signal conditioning board on the left and the Bluetooth module and microcontroller on the right. The current consumption of the Bluetooth module and

sensor board at 6 V were 35 mA and 45 mA respectively. The temperature sensors were calibrated by comparing the PT100 resistance measured with a 4 wire precision multimeter Fluke 8846A and the corresponding value calculated with the LabVIEW interface at different temperatures. The Rogowski coils were calibrated at 50 Hz as follows:

- A variac was connected to a resistive load to set different current values.
- The Rogowski coils were mounted around 36 turns of conducting wire to simulate higher currents.
- The RMS value of the current measured with a precision multimeter multiplied by the number of turns was compared with the RMS value obtained with the LabVIEW program.

The system was designed for 1.5 W power consumption, with an actual measured power of about 0.9 W. Both values are negligible compared to the power rating of the machine 7.8 kW. On top of this, the LabVIEW interface samples the input voltage and current, battery voltage and battery current in the energy harvesting module, therefore these values can be used to compensate any efficiency measurement if required.

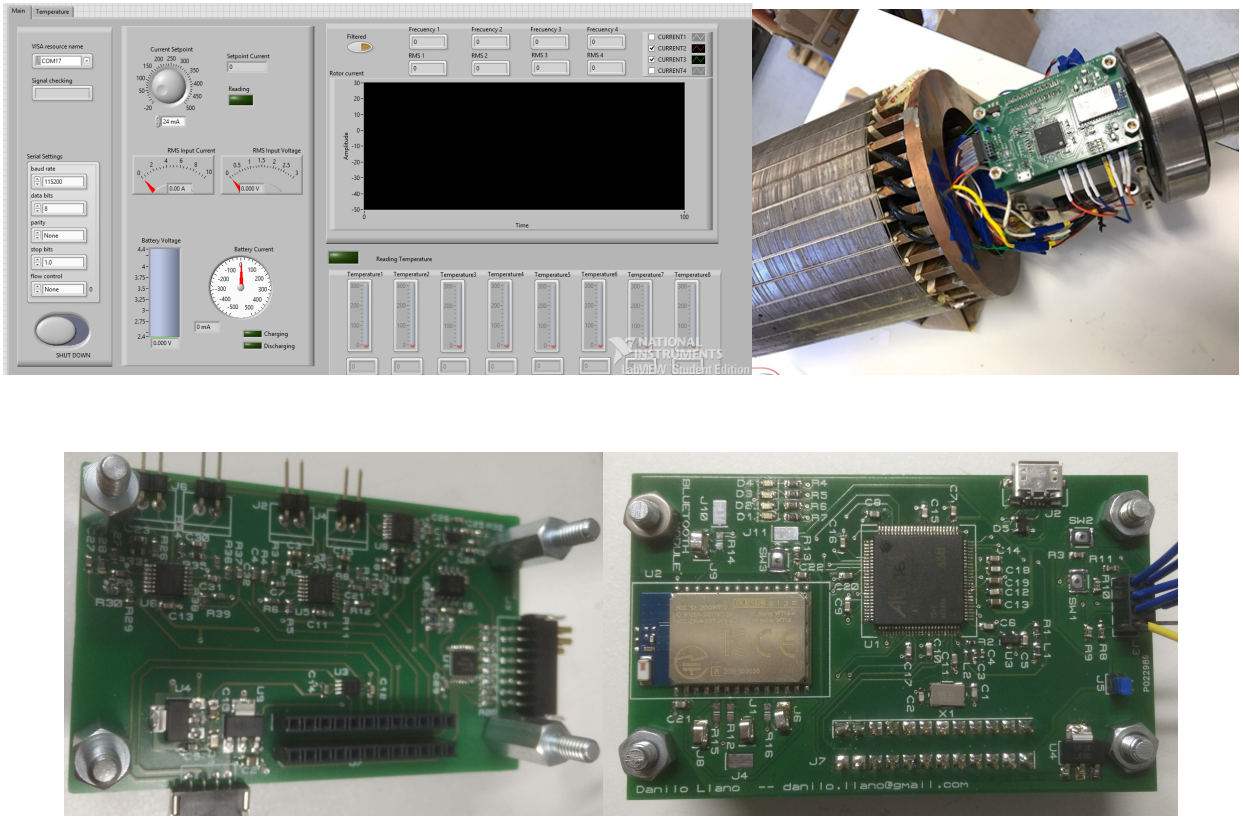


***Fig. 10.*** *Labview interface (top left), System installation (top right), Signal conditioning board (bottom left), Bluetooth module (bottom right)*

## 7. Conclusions

The aim of the paper was to demonstrate an energy harvesting system and Bluetooth module which can be mounted on the rotor of an electrical machine, in this case a BDFM, to measure and transmit

rotor current (4 channels) and temperature (8 channels). Two techniques were considered. The best solution was to insert physical taps between loops in the rotor such that small EMF voltages are induced in an external circuit. An active rectifier and DC/DC converter were designed to convert the low AC input voltage into a stable DC voltage for battery charging and powering the energy harvesting microcontroller, sensor circuitry and Bluetooth module. The system was successfully characterised (efficiency measurement) and calibrated (sensors and signal conditioning) on the laboratory bench to check it met all the design requirements. The current prototype might experience space limitations especially in compact machines with high power density, but the system could still be further miniaturised. As an example, if only temperature measurements are required the Bluetooth module and SAM4S microcontroller can be replaced with a single Bluetooth 4.0 IC featuring the same tasks but at lower sampling rates. This leads to lower power consumption, smaller electronic components, less energy storage requirement and a smaller footprint. Also, the size of the current prototype is limited by the use of components suitable for hand assembly and the presence of testing points/connectors that can be removed in further versions. Once the energy harvesting is proved to work, this current design can be optimized depending on the user specifications to reduce size and power consumption, for example if only temperature sensing is required.

## 8. Acknowledgements

The research leading to these results has received funding from the Innovate UK technology programme (Project reference number: 102155)

## 9. References

[1] E. Abdi-Jalebi and R. McMahon, "High-Performance Low-Cost Rogowski Transducers and Accompanying Circuitry," *IEEE Transactions on Instrumentation and Measurement*, vol. 56, no. 3, pp. 753–759, June 2007.

[2] P. C. Roberts, E. A. Jalebi, R. A. McMahon, and T. J. Flack, "Real-time rotor bar current measurements using Bluetooth technology for a brushless doubly fed machine (BDFM)," in *Power Electronics, Machines and Drives, 2004. (PEMD 2004). Second International Conference on (Conf. Publ. No. 498)*, vol. 1, March 2004, pp. 120–125 Vol.1.

[3] S. Abdi, E. Abdi, A. Oraee, and R. McMahon, "Equivalent Circuit Parameters for Large Brushless Doubly Fed Machines (BDFMs)," *IEEE Transactions on Energy Conversion*, vol. 29, no. 3, pp. 706–715, Sept 2014.

[4] ——, "Optimization of Magnetic Circuit for Brushless Doubly Fed Machines," *IEEE Transactions on Energy Conversion*, vol. 30, no. 4, pp. 1611–1620, Dec 2015.

[5] M. Ganchev, B. Kubicek, and H. Kappeler, "Rotor temperature monitoring system," in *Electrical Machines (ICEM), 2010 XIX International Conference on*, Sept 2010, pp. 1–5.

[6] M. Ganchev, C. Kral, H. Oberguggenberger, and T. Wolbank, "Sensorless rotor temperature estimation of permanent magnet synchronous motor," in *IECON 2011 - 37th Annual Conference on IEEE Industrial Electronics Society*, Nov 2011, pp. 2018–2023.

[7] X. Xue, V. Sundararajan, and W. P. Brithinee, "The application of wireless sensor networks for condition monitoring in three-phase induction motors," in *2007 Electrical Insulation Conference and Electrical Manufacturing Expo*, Oct 2007, pp. 445–448.

[8] G. Jianzhong, G. Hui, and H. Zhe, "Rotor temperature monitoring technology of direct-drive permanent magnet wind turbine," in *Electrical Machines and Systems, 2009. ICEMS 2009. International Conference on*, Nov 2009, pp. 1–4.

[9] M. Kovačić, M. Vražić, and I. Gašparac, "Bluetooth wireless communication and 1-wire digital temperature sensors in synchronous machine rotor temperature measurement," in *Power Electronics and Motion Control Conference (EPE/PEMC), 2010 14th International*, Sept 2010, pp. T7–25–T7–28.

[10] T. T. Toh, P. D. Mitcheson, and E. M. Yeatman, "Continuously rotating energy harvester with improved power density," *PowerMEMS, Sendai, Japan*, 2008.

[11] T. T. Toh, P. D. Mitcheson, A. S. Holmes, and E. M. Yeatman, "A continuously rotating energy harvester with maximum power point tracking," *Journal of Micromechanics and Microengineering*, vol. 18, no. 10, p. 104008, 2008.

[12] E. Abdi, R. Mcmahon, P. Malliband, S. Shao, M. E. Mathekga, P. Tavner, S. Abdi, A. Oraee, T. Long, and M. Tatlow, "Performance analysis and testing of a 250 kW medium-speed brushless doubly-fed induction generator," *IET Renewable Power Generation*, vol. 7, no. 6, pp. 631–638, Nov 2013.

[13] E. Abdi, "Modelling and instrumentation of brushless doubly-fed (induction) machines," Ph.D. dissertation, University of Cambridge, Engineering Department, 2006.

[14] D. A. Ward, "Measurement of current using Rogowski coils," in *Instrumentation in the Electrical Supply Industry, IEE Colloquium on*, Jun 1993, pp. 1/1–1/3.

[15] M. Tatlow, R. McMahon, and S. Abdi, "Wireless energy harvesting for rotor instrumentation in electrical machines," in *Power Electronics, Machines and Drives (PEMD 2016), 8th IET International Conference on*, April 2016.

[16] A. Oraee, E. Abdi, S. Abdi, and R. A. McMahon, "A study of converter rating for Brushless DFIG wind turbines," in *Renewable Power Generation Conference (RPG 2013), 2nd IET*, Sept 2013, pp. 1–4.

[17] F. Blaabjerg, R. Teodorescu, M. Liserre, and A. V. Timbus, "Overview of Control and Grid Synchronization for Distributed Power Generation Systems," *IEEE Transactions on Industrial Electronics*, vol. 53, no. 5, pp. 1398–1409, Oct 2006.

[18] J. R. Rodriguez, J. W. Dixon, J. R. Espinoza, J. Pontt, and P. Lezana, "PWM regenerative rectifiers: state of the art," *IEEE Transactions on Industrial Electronics*, vol. 52, no. 1, pp. 5–22, Feb 2005.

[19] K. Ogata, *Modern Control Engineering*. Prentice-Hall, 2010.

[20] R. D. Middlebrook and S. Cuk, "A general unified approach to modelling switching-converter power stages," in *Power Electronics Specialists Conference, 1976 IEEE*, June 1976, pp. 18–34.